Impact Modeling and Estimation for Multi-Arm Space Robot while Capturing Tumbling Orbiting Objects

Deepak Raina
Indian Institute of Technology
Jodhpur, Rajasthan 342005
raina.1@iitj.ac.in

Suril V. Shah
Indian Institute of Technology
Jodhpur, Rajasthan 342005
surilshah@iitj.ac.in

ABSTRACT

This paper presents impact modeling of a multi-arm robotic system mounted on a service satellite while capture of tumbling orbiting objects. A robotic system with multiple arms would be capable of capturing multiple objects simultaneously. Further when satellite is in broken state or does not have provision for grapple and tumbling, the interception is very difficult. In such cases, interception using multi-arm robotic system can be appealing as this will increase the probability of grasp in comparison to single-arm robot. In this paper, three phases of the capturing operation, namely, approach, impact and post impact have been modeled. In the approach phase, the end-effectors' velocities are designed same as that of the grasping point on the target in order to avoid high impact forces. But in practice, there will be a nonzero relative velocity between the end effector and the grapple point, leading to an impact. In the impact phase, a framework is developed to estimate the changes in the generalized velocities caused by the impact. In post impact phase, these velocities are used as an initial condition for the post impact dynamics simulations of the combined robotic system and target object. Efficacy of the framework is shown using a dual-arm robot mounted on a service satellite performing capturing operation for two tumbling objects.

KEYWORDS

Space Robot, Impact Modeling, Dynamic Simulation

ACM Reference format:
Deepak Raina and Suril V. Shah. 2017. Impact Modeling and Estimation for Multi-Arm Space Robot while Capturing Tumbling Orbiting Objects. In *Proceedings of AIR '17, New Delhi, India, June 28-July 2, 2017,* 6 pages.
https://doi.org/10.1145/3132446.3134896

1 INTRODUCTION

Space robotics has been an active area of research for the last few years [7, 10]. Particularly, On-Orbit Servicing (OOS) is one of the areas in space robotics that is gaining researchers' attention due to its commercial drive. There would be great demand for these OOS operations such as refueling, repair and retrieval of malfunctioning satellites, capture of debris etc. This work focuses on impact modeling while capture of debris. The entire capture operation includes three phases, namely approach, impact and post impact. The successful capture of an orbiting tumbling object using a space manipulator depends on how perfectly these three phases have been modeled.

The impact modeling has been studied widely with respect to fixed-base robots [1, 17], and various models for estimating impulse force during the collision of rigid and flexible robotic arm with environment were developed. The large impulse forces could lead to possible damage of the sytem. The various strategies for minimizing the impact forces were proposed in [5, 6, 14, 16]. In case of a multi-arm space robot, modeling and estimation of impact may not be straightforward due to the presence of the free-floating base and dynamic coupling between base and arms. Several researchers have studied impact modeling and estimation in space robots [2, 3, 8, 15]. The impact dynamics for free-floating multibody system was proposed in [15]. The work emphasized on modeling the impact dynamics of manipulator subjected to the force impulse at the hand and developed notion of the Extended-Inverse Inertia Tensor. The inertial effects during instantaneous impact duration were also taken into account by introducing the virtual rotor inertia model. Further, the impulse index and impulse ellipsoid were presented to express the magnitude and direction of force impulse, which may help in design of approach phase for minimum impact. In [2], the effect of impact due to spinning target on the dynamics of a 2-link space robot was studied, however, it was assumed that at the time of capture there is zero relative velocity between the target and the end-effector, i.e., there is no impact. Later, they studied impact considering non-zero relative velocity and also proposed the post impact control strategy using feedback linearization [3]. The impact analysis of a free-floating serial rigid body space robot was studied in [8]. The work estimated the reactions occurring at the joints and base in terms of finite velocity changes, which were then used for the post-impact motion control of the space robot.

It is worth noting that the impact modeling of multi-arm space robot is seldom reported to the best of authors' knowledge. When satellite is in broken state or does not have provision for grapple and tumbling, the capturing operation would become very difficult. In such cases, multi-arm robotic system would be very appealing as it may increase the probability of grasp in comparison to single-arm robot. Multi-arm robot can also be used to capture two or more target objects simultaneously which would enhance the capability of the space robots.

Motivated by these facts, the impact modeling and estimation is taken up in this work for multi-arm robotic systems for capture of tumbling objects. During the approach phase, the end effector of

AIR '17, June 28-July 2, 2017, New Delhi, India

ACM ISBN 978-1-4503-5294-9/17/06…$15.00
https://doi.org/10.1145/3132446.3134896

the space manipulator moves with a pre-defined trajectory which ensures zero relative velocity between end-effectors and grapple points during impact. However, it is very difficult to achieve the same in practice. When the object is tumbling, such soft approach might not exist. It may not be possible to grasp the object until its angular momentum decreases. During the impact phase, end-effector makes contact at a distinct point on the target object and impact forces are generated. These forces are modeled and estimated using conservation of momentum. The post impact phase is simulated by determining the change in generalized velocities of the end-effector and object during impact. The impact modeling of a multi-arm space robot forms the main contribution of this work. Numerical illustrations are provided using a planar dual-arm robotic system capturing two different objects.

The rest of the paper is organized as follows: Equations-of-motion (EOM) for free-floating robot and orbiting objects are presented in Section II. Modeling of three phases of capturing operation namely approach, impact and post impact are presented in Section III, while the implementation of the proposed framework on dual arm space robot is presented in Section IV. Finally, conclusions are given in Section V.

2 EQUATIONS-OF-MOTION

In this section, the EOM for a multi-arm robot mounted on a service satellite and a tumbling orbiting objects are presented. These equations are obtained using Euler-Lagrange formulation [12].

2.1 Dynamics of Multi-Arm Robot

The EOM for a multi-arm n-Degrees-Of-Freedom (n-DOF) robotic system mounted on a floating-base as shown in Fig. 1, is written as

$$\begin{bmatrix} \boldsymbol{I}_b & \boldsymbol{I}_{bm} \\ \boldsymbol{I}_{bm}^T & \boldsymbol{I}_m \end{bmatrix} \begin{bmatrix} \dot{\boldsymbol{t}}_b \\ \ddot{\boldsymbol{\theta}} \end{bmatrix} + \begin{bmatrix} \boldsymbol{c}_b \\ \boldsymbol{c}_m \end{bmatrix} = \begin{bmatrix} \boldsymbol{F}_b \\ \boldsymbol{\tau}_m \end{bmatrix} + \begin{bmatrix} \boldsymbol{J}_{be}^T \\ \boldsymbol{J}_{me}^T \end{bmatrix} \boldsymbol{F}_e \quad (1)$$

where
$\boldsymbol{I}_b \in R^{6\times6}$ and $\boldsymbol{I}_m = diag\left[\boldsymbol{I}_{m1} \quad \dots \quad \boldsymbol{I}_{mi} \quad \dots \quad \boldsymbol{I}_{mr}\right] \in R^{n\times n}$ are the inertia matrices of the base and manipulators, respectively,
$\boldsymbol{I}_{bm} = \left[\boldsymbol{I}_{bm1} \quad \dots \quad \boldsymbol{I}_{bmi} \quad \dots \quad \boldsymbol{I}_{bmr}\right] \in R^{6\times n}$ is the coupling inertia matrix,
$\dot{\boldsymbol{t}}_b = \left[\dot{\boldsymbol{\omega}}_b^T \quad \dot{\boldsymbol{v}}_b^T\right]^T \in R^{6\times1}$ is the vector of angular and linear accelerations of the base,
$\ddot{\boldsymbol{\theta}} = \left[\ddot{\boldsymbol{\theta}}_1^T \quad \dots \quad \ddot{\boldsymbol{\theta}}_{\boldsymbol{i}}^T \quad \dots \quad \ddot{\boldsymbol{\theta}}_r^T\right]^T \in R^{n\times1}$ is the vector of joint accelerations,
$\boldsymbol{c}_b \in R^{6\times1}$ and $\boldsymbol{c}_m = \left[\boldsymbol{c}_{m1}^T \quad \dots \quad \boldsymbol{c}_{mi}^T \quad \dots \quad \boldsymbol{c}_{mr}^T\right]^T \in R^{n\times1}$ are the velocity dependent nonlinear terms associated with the base and manipulator, respectively,
$\boldsymbol{F}_b \in R^{6\times1}$ and $\boldsymbol{F}_e \in R^{6r\times1}$ are the vectors of moments and forces exerted on the centroid of base and end-effectors, respectively,
$\boldsymbol{\tau}_m = \left[\boldsymbol{\tau}_{m1}^T \quad \dots \quad \boldsymbol{\tau}_{mi}^T \quad \dots \quad \boldsymbol{\tau}_{mr}^T\right]^T \in R^{n\times1}$ is the vector of manipulator joint torques and
$\boldsymbol{J}_{be} \in R^{6r\times6}$and $\boldsymbol{J}_{me} \in R^{6r\times n}$ are the Jacobian matrices for the base and manipulator, respectively.

It may be noted that $\boldsymbol{I}_{mi}$ is the inertia matrix, $\boldsymbol{I}_{bmi}$ is the coupling inertia matrix, $\boldsymbol{c}_{mi}$ is the velocity dependent non-linear term, $\boldsymbol{\tau}_{mi}$ is the joint torque and $\ddot{\boldsymbol{\theta}}_i = \left[\ddot{\theta}_{1i} \quad \dots \quad \ddot{\theta}_{ki} \quad \dots \quad \ddot{\theta}_{ni}\right]^T$ is the vector of joint accelerations for the i^{th} arm.

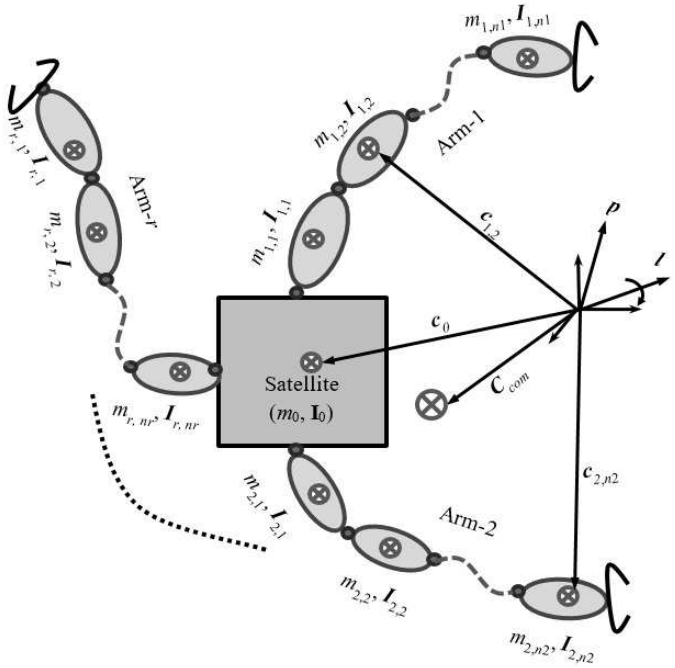

Figure 1: A multi-arm robotic system mounted on a service satellite. The robot has r arms and the j_{th} arm has n_j links and n_j joints. Mass and inertia tensor of the k_{th} link on the j_{th} arm are denoted by $m_{j,k}$ and $I_{j,k}$, respectively. p and l are the linear and angular momenta, respectively. The total degree of freedom of the system is $n_1 + \dots + n_r = n$

The reduced form of the EOM of free-floating robot [8] would be used for modeling impact. The reduced form can be obtained by omitting base acceleration $\dot{\boldsymbol{t}}_b$ from (1), as:

$$\boldsymbol{I}\ddot{\boldsymbol{\theta}} + \boldsymbol{c} = \boldsymbol{\tau} + \boldsymbol{J}^T\boldsymbol{F}_e \quad (2)$$

where $\boldsymbol{I} = \boldsymbol{I}_m - \boldsymbol{I}_{bm}^T\boldsymbol{I}_b^{-1}\boldsymbol{I}_{bm}$ is the Generalized Inertia Matrix (GIM), $\boldsymbol{c} = \boldsymbol{c}_m - \boldsymbol{I}_{bm}^T\boldsymbol{I}_b^{-1}\boldsymbol{c}_b$ is the Generalized Coriolis and centrifugal force, $\boldsymbol{\tau} = \boldsymbol{\tau}_m - \boldsymbol{I}_{bm}^T\boldsymbol{I}_b^{-1}\boldsymbol{F}_b$ is the Generalized torque and $\boldsymbol{J}^T = \boldsymbol{J}_{me}^T - \boldsymbol{I}_{bm}^T\boldsymbol{I}_b^{-1}\boldsymbol{J}_{be}^T$ is the Generalized Jacobian Matrix (GJM) [9, 13] for the free-floating robot.

2.2 Target Dynamics

In this paper, it is assumed that at a given instant of time, r manipulators capture r objects. These objects are modeled as free-floating rigid bodies.

The EOM for r-targets can be written as:

$$\boldsymbol{I}_t\dot{\boldsymbol{t}}_t = \boldsymbol{\tau}_t - \boldsymbol{J}_t^T\boldsymbol{F}_e \quad (3)$$

where $\boldsymbol{\tau}_t \in R^{6r\times1}$ is the vector of generalized moments and forces exerted on target object, $\boldsymbol{I}_t \in R^{6r\times6r}$ is the inertia matrix, $\dot{\boldsymbol{t}}_t \in R^{6r\times1}$ is the linear and angular acceleration vector and $\boldsymbol{J}_t \in$

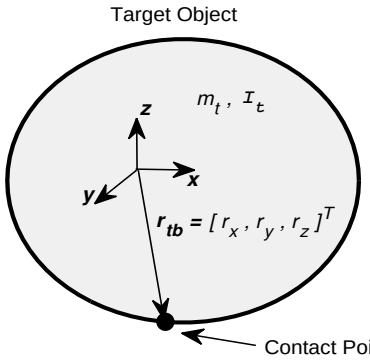

Figure 2: A free-floating target object

$R^{6r\times 6r}$ is the Jacobian for r-objects. The $\boldsymbol{I}_t$, $\dot{\boldsymbol{t}}_t$ and $\boldsymbol{J}_t$ in case of r-targets can be written as:

$$\begin{aligned} \boldsymbol{I}_t &= diag\begin{bmatrix}\boldsymbol{M}_{t1} & \dots & \boldsymbol{M}_{ti} & \dots & \boldsymbol{M}_{tr}\end{bmatrix} \\ \dot{\boldsymbol{t}}_t &= \begin{bmatrix}\dot{\boldsymbol{t}}_{t1}^T & \dots & \dot{\boldsymbol{t}}_{ti}^T & \dots & \dot{\boldsymbol{t}}_{tr}^T\end{bmatrix}^T \\ \boldsymbol{J}_t &= diag\begin{bmatrix}\boldsymbol{J}_{t1} & \dots & \boldsymbol{J}_{ti} & \dots & \boldsymbol{J}_{tr}\end{bmatrix} \end{aligned} \tag{4}$$

where

$$\begin{aligned} \boldsymbol{M}_{ti} &= \begin{bmatrix} \boldsymbol{\mathcal{I}}_t & \boldsymbol{O} \\ \boldsymbol{O} & m_t\boldsymbol{1}\end{bmatrix}_i \\ \dot{\boldsymbol{t}}_{\boldsymbol{t}\boldsymbol{i}} &= \begin{bmatrix}\dot{\boldsymbol{\omega}}_t^T & \dot{\boldsymbol{\upsilon}}_t^T\end{bmatrix}_i^T \\ \boldsymbol{J}_{ti} &= \begin{bmatrix} \boldsymbol{1} & \boldsymbol{O} \\ \boldsymbol{R}_{tb} & \boldsymbol{1}\end{bmatrix}_i \end{aligned} \tag{5}$$

In (5), m_t is the mass and $\boldsymbol{\mathcal{I}}_t \in R^{3\times 3}$ is the centroidal inertia tensor of the i^{th} object, $\boldsymbol{1} \in R^{3\times 3}$ is identity matrix and $\boldsymbol{O}$ is the null matrix of compatible dimension. $\boldsymbol{\omega}_t \in R^{3\times 1}$ and $\boldsymbol{\upsilon}_t \in R^{3\times 1}$ are the angular and linear velocity vectors of i^{th} target, respectively. $\boldsymbol{R}_{tb}$ is the cross-product tensor associated with $\boldsymbol{r}_{tb}$, which is the position vector from center-of-mass (COM) of the i^{th} target to the point of contact as shown in Fig. 2.

3 IMPACT MODEL

The following assumptions are made while modeling impact dynamics of the multi-arm space robot:

(1) The time duration of impact is so short (approximately 10^{-3} s) that the generalized position coordinates of the system remain same over the impact duration, while the generalized velocities change substantially.
(2) The effect of other forces except the impact force can be disregarded. From this assumption, we can say that the inertia term of dynamic equation is dominant and other terms are less important for the system dynamics at impact.

3.1 Pre-Impact Phase

In order to capture the target, the end-effector has to move from its initial pose (position and orientation) to the capture point. In the case of tumbling target, the end-effector begins with zero velocity and approaches with the prescribed final velocity. For this the independent joint velocities are designed using a fourth order interpolating polynomial as follows:

$$\dot{\boldsymbol{\theta}}_k(t) = \frac{\theta_k(T) - \theta_k(0)}{T}\left[a\left(\frac{t}{T}\right)^2 + b\left(\frac{t}{T}\right)^3 + c\left(\frac{t}{T}\right)^4\right] \tag{6}$$

where

$$a = 3(-4s + 10),\ b = 4(7s - 15),\ c = 5(-3s + 6)$$

$$s = \frac{\dot{\theta}_k(T)}{\frac{\theta_k(T)-\theta_k(0)}{T}} \tag{7}$$

The above trajectory ensures zero initial velocity and acceleration and zero final acceleration, whereas final velocity is $\dot{\theta}_k(T)$ for the k^{th} joint on i^{th} arm. The trajectory requires initial $\theta_k(0)$ and final $\theta_k(T)$ positions as the inputs.

3.2 Impact Phase

The Impact modeling for 2 link robot has already been proposed in [2]. This model has been extended for impact modeling of multi-arm space robot with multiple target objects. To model the impact phase, let us consider that the target object collides with the end effector of the robot arm mounted on a service satellite at a known single point and as a result of this collision, impact force $\boldsymbol{F}_e$ is induced.

By combining (2) and (3), the impact force $\boldsymbol{F}_e$ can be eliminated to obtain the following equation:

$$\boldsymbol{J}^T\boldsymbol{J}_t^{-T}\boldsymbol{I}_t\dot{\boldsymbol{t}}_t + \boldsymbol{I}\ddot{\boldsymbol{\theta}} = -\boldsymbol{c} + \boldsymbol{\tau} + \boldsymbol{J}^T\boldsymbol{J}_t^{-T}\boldsymbol{\tau}_t \tag{8}$$

Let the duration of impact be T seconds. Now (8) would be integrated over T time period. Before integrating, one can recall the assumption (1) that all of the generalized position coordinates of the system remain same over this period, although the generalized velocities and accelerations may change. Since $\boldsymbol{J}, \boldsymbol{J}_t, \boldsymbol{I}_t, \boldsymbol{I}$ depend only on the position coordinates, these matrices would remain constant and thus can be taken out of the integral. Also, the impact force is usually very large and acts for a very short time T. Thus one can say that [2]

$$\begin{aligned} \boldsymbol{T} &= O(\epsilon),\ where\ \epsilon << 1 \\ \dot{\boldsymbol{\theta}}, \boldsymbol{t}_t &= O(1) \\ \ddot{\boldsymbol{\theta}}, \dot{\boldsymbol{t}}_t &= O(1/\epsilon) \end{aligned} \tag{9}$$

Now, integration of (8) over time period T would give:

$$\begin{aligned} &\boldsymbol{J}^T\boldsymbol{J}_t^{-T}\boldsymbol{I}_t(\boldsymbol{t}_{tf} - \boldsymbol{t}_{ti}) + \boldsymbol{I}(\dot{\boldsymbol{\theta}}_f - \dot{\boldsymbol{\theta}}_i) \\ &= \int_0^T [-\boldsymbol{c} + \boldsymbol{\tau} + \boldsymbol{J}^T\boldsymbol{J}_t^{-T}\boldsymbol{\tau}_t]dt \end{aligned} \tag{10}$$

where the subscripts f and i stand for values after and before the impact, respectively. Clearly, the left-hand side of (10) is $O(1)$. The integrand on the right-hand side is also $O(1)$; however, the interval of the integration is of $O(\epsilon)$ and, hence, the right-hand side is of $O(\epsilon)$ and can be ignored compared to the left-hand side. Thus (10) can be written as

$$\boldsymbol{J}^T\boldsymbol{J}_t^{-T}\boldsymbol{I}_t(\boldsymbol{t}_{tf} - \boldsymbol{t}_{ti}) + \boldsymbol{I}(\dot{\boldsymbol{\theta}}_f - \dot{\boldsymbol{\theta}}_i) = 0 \tag{11}$$

The above equation represents conservation of generalized momenta and is valid for all collisions.

To calculate magnitude of impulse, (2) is then rearranged and integrated over time duration of impact T as

$$\overline{F} = J^{-T} I(\dot{\theta}_f - \dot{\theta}_i) \tag{12}$$

3.3 Post-Impact Phase

The post impact dynamics depends on the fact that the impact is inelastic or elastic. In case of inelastic impact, the two systems become rigidly attached to each other after impact at the contact points, whereas in the case of elastic impact, the systems rebound with no loss of energy. In this paper, impact is assumed to be inelastic and is modeled for capturing and berthing operations.

In plastic impact, the velocity of end effector and contact point would be same, i.e.,

$$J\dot{\theta}_f = J_t t_{tf} \tag{13}$$

The generalized velocities of the target can be written in terms of manipulator velocities to get

$$t_{tf} = J_t^{-1} J\dot{\theta}_f \tag{14}$$

Substitution of (14) into (11) yields

$$\dot{\theta}_f = G^{-1} H \tag{15}$$

where

$$G = J^T J_t^{-T} I_t J_t^{-1} J + I$$
$$H = J^T J_t^{-T} I_t t_{ti} + I\dot{\theta}_i \tag{16}$$

From (15) we can obtain final velocities for space robot, which can be used to calculate change in target velocities using (14). The final base velocities $\dot{t}_{bf}$ can be obtained using the momentum equation [4] as given by

$$\dot{t}_{bf} = I_b^{-1}\left(\begin{bmatrix} p \\ l - c_o \times p \end{bmatrix} - I_{bm}\dot{\theta}_f\right) \tag{17}$$

From (15) and (17) we get generalized velocity vector as an initial condition for the post impact dynamic simulations.

4 RESULTS AND DISCUSSION

A 3-link dual arm robot mounted on a service satellite has been choosen as an example for performing numerical experiments. The solid sphere rotating about its z-axis has been considered as a target object. The link length, mass and inertia properties of the base and robot, used for the purpose of simulation, are provided in Table 1. The COM of the satellite is located at $(0, 0)$. The mass, mass moment of inertia (MOI) and location of two target objects are given in Table 2. In the numerical experiments, three phases of impact are modeled and the behaviour of the system undergoing impact is estimated.

In the approach phase, the trajectory in (6) requires initial and final joint angles as the inputs, which are given in Table 3. These initial and final joint angles are obtained using inverse kinematics relationships. The Initial and final positions for both end-effectors are given in Table 4. The final position will be the point of contact on the target sphere. Moreover (6) also requires final joint velocities which can be obtained using the GJM. The end-effectors' velocities are taken as 0.1 m/s in -X directions for end-effector 1 and in +X direction for end-efffector 2. Both the targets are assumed to have angular velocity of 0.2 rad/s in anti-clockwise direction. This is considered as Case 1. The pre-impact simulations were carried out using Recursive Dynamic Simulator (ReDySim) [11] for the time period of 20s. The trajectory following Proportional and Derivative (PD) control law given by (17) was used for carrying out dynamic simulations.

$$\tau = K_p(\theta_d - \theta) + K_v(\dot{\theta}_d - \dot{\theta}) \tag{18}$$

where, K_p and K_d are the diagonal matrices of proportional and derivative gains and $\dot{\theta_d}$ and $\dot{\theta}$ are desired and actual joint velocities, respectively. The pre-impact and impact phase simulation results are shown in Figs. 3 and 4. The joints angles achieved during forward dynamics simulation in approach phase are shown in Fig. 5. The velocity of end effector of robot arms is shown in Fig. 6. The total momentum of the system before impact is shown in Fig. 7. It is evident from Fig. 6 that end-effector won't be able to reach prescribed velocity of 0.1 m/s. The velocity conditions at the time of impact are clearly shown in the Fig. 8. This velocity difference would cause impact at the contact point.

In the Impact phase, (13-17) were used to model impact and estimate the change in velocities of the robot and target. The generalized velocity vector so obtained was used as an initial condition for post dynamic simulations. Since we assumed that the target is captured rigidly by the end effector as a perfectly inelastic case,

Table 1: Model parameters of dual-arm robot and base

	Base	Robot					
		Arm 1			Arm 2		
Link	0	1	2	3	4	5	6
Length (m)	1	1	1	1	1	1	1
Mass (kg)	500	10	10	10	10	10	10
MOI (kg-m^2)	83.61	1.05	1.05	1.05	1.05	1.05	1.05

Table 2: Model parameters of target

	Target 1	Target 2
Mass (kg)	10	10
Radius (m)	0.5	0.5
MOI (kg-m^2)	1	1
Location (m)	(2,-2)	(-2,2)

Table 3: Desired initial and final joint angles

	Arm 1			Arm 2		
	θ_1	θ_2	θ_3	θ_4	θ_5	θ_6
Initial	0.698	-1.571	1.047	2.444	1.571	-1.047
Final	-0.524	-1.393	-0.035	2.618	-1.393	-0.035

Table 4: Initial and final end-effectors' position

	P_{e1x}	P_{e1y}	P_{e2x}	P_{e2y}
Initial	2.9	0.05	-2.9	0.05
Final	2	-1.5	-2	1.5

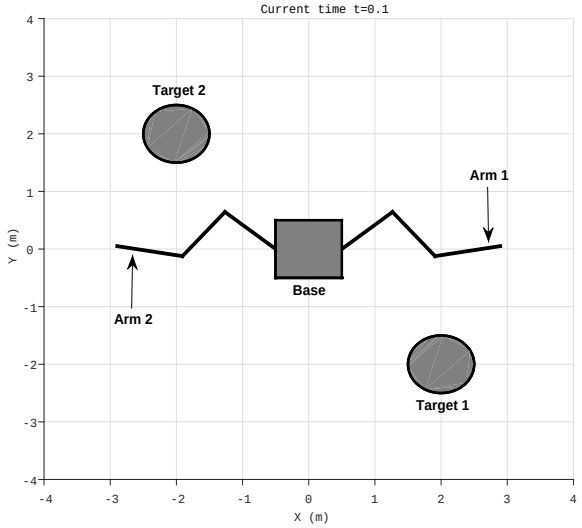

Figure 3: Pre-impact initial configuration

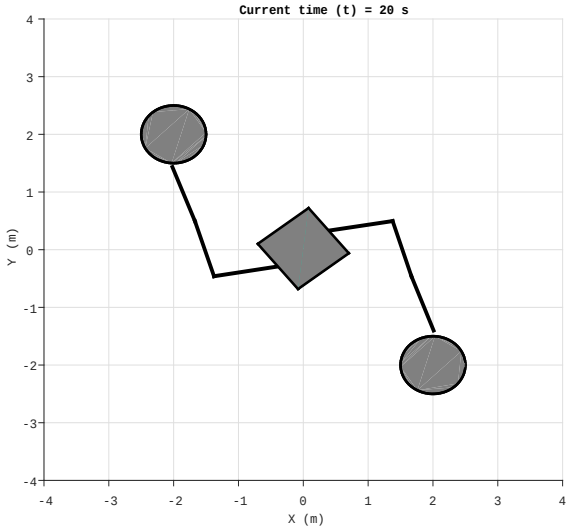

Figure 4: Impact phase configuration

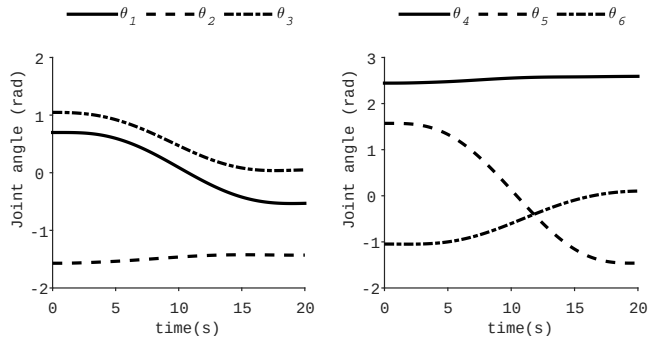

Figure 5: Actual joint angles

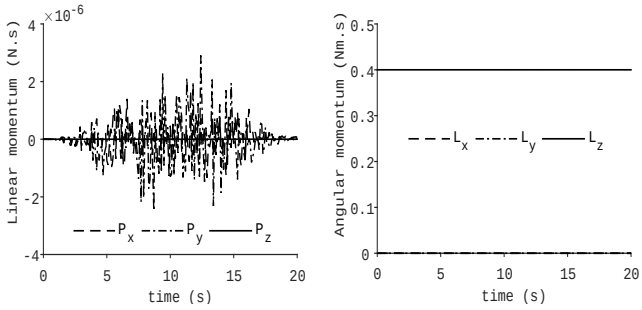

Figure 7: Total momentum before impact

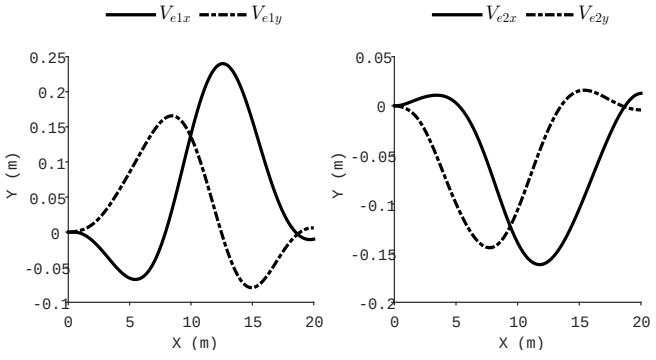

Figure 6: End-effector velocity

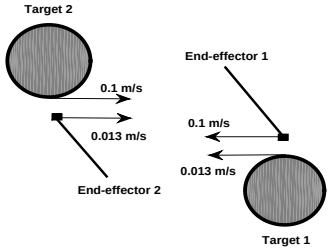

Figure 8: Impact phase velocities

so the robot and target would become one system in post-impact phase. The post impact simulations were also carried out using ReDySim [11] for 50s. Further, two more cases when both targets are stationary (Case 2) and when target 1 and 2 have angular velocity of 0.2 rad/sec and -0.2 rad/sec respectively (Case 3), were simulated.

The post impact dynamic simulations for the above mentioned 3 cases are shown in Fig. 9. The Magnitude of impulse in these cases is shown in Table 5. The impact force can be calculated by multiplying this impulse force with time duration of impact. The total momentum of the system for Case 1 after impact is shown in the Fig. 10.

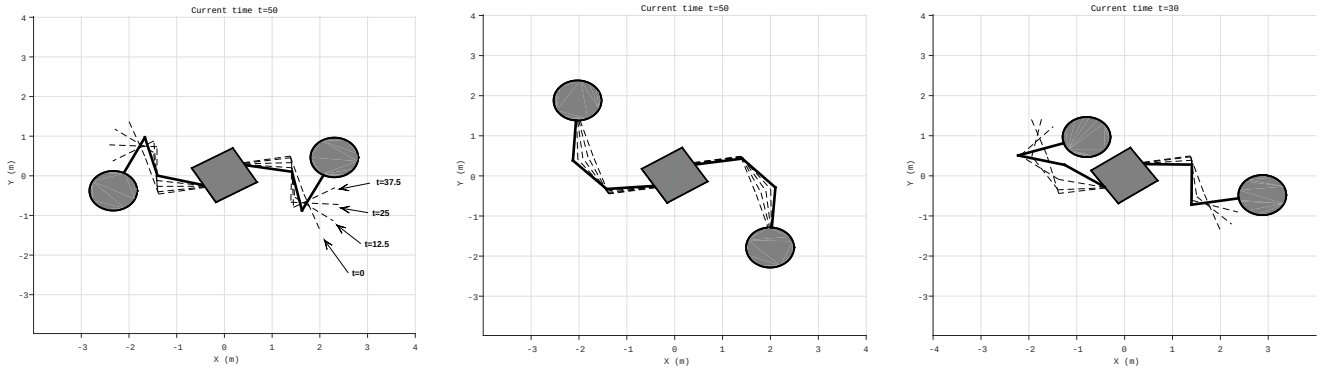

(a) Both target rotating in same direction (b) Both target stationary (c) Both target rotating in opposite direction

Figure 9: Post-impact simulation

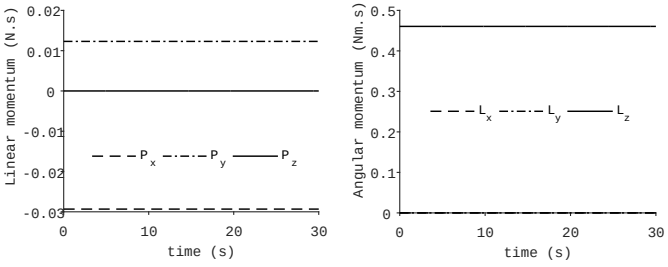

Figure 10: Total momentum after impact

Table 5: Impulse (N-s) estimation

Case	Impulse ($\overline{F}$)	
	Contact Point 1	Contact Point 2
Case 1	0.0873	0.0873
Case 2	0.0131	0.0131
Case 3	0.0873	0.0873

It is evident from the Figs. 7 and 10 that total momentum of the system is almost same before and after impact. Thus the laws of inelastic collision are satisfied.

5 CONCLUSIONS

In this work, a framework for impact modeling and estimation of a multi-arm space robot has been presented for capturing a tumbling orbiting object. The impact of two orbiting targets with two arms of a space robot have been modeled and post impact dynamics of a dual-arm space robot and target has been simulated. It may be noted that post impact uncontrolled dynamics will result in undesirable motion, thus a control scheme will be proposed to achieve post-impact stabilization in future work. Experimental implementation and validation of the proposed method on an earth-based dual-arm robot will also be carried out in future.

REFERENCES

[1] BV Chapnik, Glenn R Heppler, and J Dwight Aplevich. 1991. Modeling impact on a one-link flexible robotic arm. *IEEE Transactions on Robotics and Automation* 7, 4 (1991), 479–488.

[2] Xavier Cyril, Gilbert J Jaar, and Arun K Misra. 1993. The effect of payload impact on the dynamics of a space robot. In *Intelligent Robots and Systems' 93, IROS'93. Proceedings of the 1993 IEEE/RSJ International Conference on*, Vol. 3. IEEE, 2070–2075.

[3] Xavier Cyril, Arun K Misra, Michel Ingham, and Gilbert J Jaar. 2000. Postcapture dynamics of a spacecraft-manipulator-payload system. *Journal of Guidance, Control, and Dynamics* 23, 1 (2000), 95–100.

[4] A Gattupalli, SV Shah, K Madhava Krishna, and AK Misra. 2013. Control strategies for reactionless capture of an orbiting object using a satellite mounted robot. In *Proceedings of Conference on Advances In Robotics*. ACM, 1–6.

[5] Matthew W Gertz, Jin-Oh Kim, and Pradeep K Khosla. 1991. Exploiting redundancy to reduce impact force. In *Intelligent Robots and Systems' 91.'Intelligence for Mechanical Systems, Proceedings IROS'91. IEEE/RSJ International Workshop on*. IEEE, 179–184.

[6] ZC Lin, Rajni V Patel, and Constantinos A Balafoutis. 1995. Impact reduction for redundant manipulators using augmented impedance control. *Journal of Field Robotics* 12, 5 (1995), 301–313.

[7] J-C Liou. 2011. An active debris removal parametric study for LEO environment remediation. *Advances in Space Research* 47, 11 (2011), 1865–1876.

[8] Dragomir N Nenchev and Kazuya Yoshida. 1999. Impact analysis and post-impact motion control issues of a free-floating space robot subject to a force impulse. *IEEE Transactions on Robotics and Automation* 15, 3 (1999), 548–557.

[9] Subir Kumar Saha. 1996. A unified approach to space robot kinematics. *IEEE transactions on robotics and automation* 12, 3 (1996), 401–405.

[10] Florian Sellmaier, Toralf Boge, Jörn Spurmann, Sylvain Gully, Thomas Rupp, and Felix Huber. 2010. On-orbit servicing missions: Challenges and solutions for spacecraft operations. In *SpaceOps 2010 Conference Delivering on the Dream Hosted by NASA Marshall Space Flight Center and Organized by AIAA*. 2159.

[11] Suril V Shah, Paramanand V Nandihal, and Subir K Saha. 2012. Recursive dynamics simulator (ReDySim): A multibody dynamics solver. *Theoretical and Applied Mechanics Letters* 2, 6 (2012).

[12] Mark W Spong, Seth Hutchinson, and Mathukumalli Vidyasagar. 2006. *Robot modeling and control*. Vol. 3. Wiley New York.

[13] Yoji Umetani and Kazuya Yoshida. 1989. Resolved motion rate control of space manipulators with generalized Jacobian matrix. *IEEE Transactions on robotics and automation* 5, 3 (1989), 303–314.

[14] Ian D Walker. 1994. Impact configurations and measures for kinematically redundant and multiple armed robot systems. *IEEE transactions on robotics and automation* 10, 5 (1994), 670–683.

[15] Kazuya Yoshida and Naoki Sashida. 1993. Modeling of impact dynamics and impulse minimization for space robots. In *Intelligent Robots and Systems' 93, IROS'93. Proceedings of the 1993 IEEE/RSJ International Conference on*, Vol. 3. IEEE, 2064–2069.

[16] Kamal Youcef-Toumi and David A Gutz. 1989. Impact and force control. In *Robotics and Automation, 1989. Proceedings., 1989 IEEE International Conference on*. IEEE, 410–416.

[17] Yuan-Fang Zheng and Hooshang Hemami. 1985. Mathematical modeling of a robot collision with its environment. *Journal of Field Robotics* 2, 3 (1985), 289–307.